Polymer 50 (2009) 347–356

Contents lists available at ScienceDirect

Polymer

journal homepage: www.elsevier.com/locate/polymer

Feature Article

Structure–mechanical property correlations of model siloxane elastomers with controlled network topology

Kenji Urayama [a,*], Takanobu Kawamura [b], Shinzo Kohjiya [c]

[a] Department of Materials Chemistry, Kyoto University, Kyoto 615-8510, Japan
[b] Department of Chemical Engineering, Kanazawa University, Ishikawa 920-1192, Japan
[c] Department of Chemistry, Mahidol University, Phuthamonthon, Nakorn Pathom 73170, Thailand

ARTICLE INFO

Article history:
Received 6 September 2008
Received in revised form
16 October 2008
Accepted 21 October 2008
Available online 29 October 2008

Keywords:
Elastomers
Polydimethylsiloxane
Rubber elasticity
Viscoelasticity

ABSTRACT

We review our recent studies towards the molecular understanding of mechanical properties–structure relationships of elastomers using model polydimethylsiloxane (PDMS) networks with controlled topology. The model elastomers with controlled lengths of the network strands and known amounts of cross-links and dangling chains are obtained by end-linking the functionally terminated precursor PDMS with known molecular weights using multi-functional cross-linkers. Several modern entanglement theories of rubber elasticity are assessed in an unambiguous manner on the basis of the nonlinear stress–strain behavior of the model elastomers under general biaxial strains. The roles of cross-links and entanglements in the large-scale structure of the swollen state are revealed from small angle X-ray scattering spectra. A remarkably stretchable elastomer with the ultimate strain over 3000% is obtained by optimizing the network topology for high extensibility, i.e., by reducing the amounts of trapped entanglements and the end-to-end distance of the network strands. The model elastomers with unattached chains exhibit a pronounced viscoelastic relaxation originating from the relaxation by reptative motion of the guest chains. The relaxation spectra provide a definite basis to discuss the dynamics of guest linear chains trapped in fixed polymer networks. The temperature- and frequency-insensitive damping elastomers are made by introducing intentionally many dangling chains into the networks.

1. Introduction

Elastomers exhibit large reversible deformabilities with distinctly low elastic modulus – which are unparalleled in solid materials – due to the entropic elasticity. Such unique mechanical properties of elastomers originate from the three-dimensional network structure comprising long and flexible polymer chains [1,2]. The amorphous network structure of elastomers is characterized by several topological parameters such as the length of the network strands, functionality of cross-links, and the amounts of entanglements, dangling chains and loops. Extensive research on elastomers has been conducted over the years, and today, elastomers are widely utilized as commercial products. However, the molecular understanding of the network topology–mechanical property relationships still remains incompletely understood. This is primarily because conventional elastomers formed by random cross-linking methods have very obscure structure with a broad network strand length distribution and an unknown number of dangling chains. Well-characterized model elastomers with known structural parameters can be prepared by the end-linking reaction [2–6]. Functionally terminated precursor chains with known molecular masses are end-linked with cross-linkers of functionality three or more (Fig. 1). The length of the network strands between the cross-links can be controlled by the length of the precursor chains. A finite imperfection in the end-linking reaction invalidates the equivalence of the lengths of the precursor chains and network strands, and this deviation can be quantitatively evaluated on the basis of a nonlinear polymerization model [7] and the quantity of unreacted materials extracted after the reaction. Similarly, the size distribution of the network strands can be controlled by the size distribution of the precursor chains. For example, the end-linking of mixtures of short and long precursor chains resulted in elastomers with bimodal length distribution of network strands [2,5,8]. The trimodal [9] or "pseudo unimodal" (extremely broad unimodal) [5] length distribution of network strands is also possible. Moreover, dangling chains (those tethered to the network at only one end) can be introduced intentionally by using mixtures of mono-functional and bi-functional precursors [2,4,10]. The end-linking of precursors in the solution can vary the amount of trapped entanglements in the resultant elastomers by changing the precursor concentration [11–13]. The end-linking

* Corresponding author.
E-mail address: urayama@rheogate.polym.kyoto-u.ac.jp (K. Urayama).

0032-3861/$ – see front matter © 2008 Elsevier Ltd. All rights reserved.
doi:10.1016/j.polymer.2008.10.027

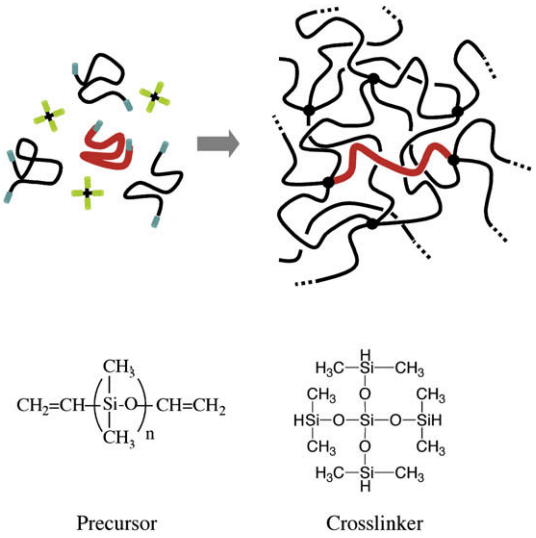

Fig. 1. End-linking telechelic precursors with tetra-functional cross-linkers.

reaction provides the mechanism to fabricate elastomers with a rich variety of topological characteristics.

Poly(dimethylsiloxane) (PDMS) is known as one of the most flexible polymers [14]. The high flexibility of PDMS originates from the structural features of the Si–O bonds; they have a longer bond length, larger bond angle, and significantly lower torsional potential than C–C bonds. This leads to a very low glass transition temperature (ca. −120 °C) for PDMS. PDMS undergoes crystallization at considerably low temperatures of below −30 °C. Usually, crosslinked PDMS does not exhibit strain-induced crystallization at room temperature. These features of PDMS are beneficial for fundamental studies of rubber elasticity. In fact, PDMS has often been employed as a precursor in end-linked elastomers. There are several types of chemical reaction that facilitate end-linking. The addition reaction between vinyl groups and Si–H groups by the use of a Pt catalyst is one of the most well-known reactions (Fig. 1). This reaction was employed for sample preparation in all our studies introduced in this article.

In this article, we review our recent studies on different types of PDMS elastomers with controlled network topology. Section 2 describes the nonlinear elasticity of model elastomers under general biaxial strains. Several modern entanglement theories for rubber elasticity are strictly assessed using stress–strain data obtained in different types of deformations. Section 3 discusses a large-scale structure present in the swollen model elastomers with controlled lengths of network strands on the basis of small angle X-ray scattering spectra. Section 4 introduces that the remarkably extensible elastomers with the unusual network topology tuned to high extensibility which are prepared by end-linking in semi-dilute solutions and subsequently drying. Section 5 describes the viscoelastic properties of the model elastomers with low concentration of unattached chains and model irregular elastomers with a known amount of dangling chains. The model elastomers with low concentrations of unattached chains provide a basis for discussion of the dynamics of free guest chains in fixed (crosslinked) polymer networks. The model irregular elastomers with a known amount of dangling chains result in an elastomer with high damping, which is insensitive to temperature and frequency.

2. Nonlinear elasticity characterized by general biaxial strains

Elastomers exhibit large (and recoverable) deformabilities due to small forces. The relation between stress and strain is linear only at very small strains, and it is significantly nonlinear at moderate and large strains. Uniaxial deformation has often been employed to characterize nonlinear elasticity because of its experimental simplicity. Uniaxial deformation, however, is one of the different types of deformations, and it provides limited information about nonlinear elasticity. In contrast, general biaxial strains that vary independently in two orthogonal directions (Fig. 2) cover the entire range of physically accessible deformations in incompressible elastomers [1,15,16]. The significance of general biaxial strains was recognized a long time ago, but there are few corresponding experiments [17–19] due to the complexity of the instruments required. Several researchers [1,16,20–24] have stated that analysis relying only on uniaxial data often leads to an erroneous understanding of nonlinear rubber elasticity – however, this important fact appears to be largely neglected. A typical example is the overestimation of the familiar Mooney–Rivlin plot using uniaxial data: the linearity in this plot is often superficial because the free energy estimated from this plot does not describe the biaxial data [20–24].

The biaxial data of well-characterized elastomers provide a definite basis for the molecular understanding of rubber elasticity. Many entanglement models have been proposed to improve the flaws in the classical theories [5]: the classical theories consider neither the topological interaction (entanglement effect) arising due to the uncrossability of network strands nor their finite extensibility. Most of the past assessments of these entanglement theories relied only on uniaxial data. Uniaxial deformation is not sensitive enough to distinguish one model from another [21,25]. In addition, the structural parameters in the models are often treated as additional fitting parameters because of obscurity of structural parameters of the randomly crosslinked elastomer samples. This treatment lends more ambiguity to the assessments. We investigated the nonlinear stress–strain relations of the model elastomers of end-linked PDMS under general biaxial deformations by using a custom-built tester to obtain an unambiguous basis for testing the theories [23,24,26–28]. The typical size of square sheet samples is ca. 50 mm width and ca. 1 mm thickness. The precursor PDMS chains used are highly entangled before end-linking due to the high molecular weight ($M_w = 89{,}500$). This molecular weight is considerably larger than the critical molecular weight for the formation of entanglement couplings ($M_c \approx 17{,}000$) [29] as well as the molecular weight between adjacent entanglements ($M_e \approx 10{,}000$) [30]. The mesh of the resultant networks is dominated by trapped entanglements instead of chemical cross-links. The PDMS elastomers with various amounts of trapped entanglements were prepared by varying the weight fraction of precursor PDMS (ϕ_0) in the solutions at end-linking. An oligodimethylsiloxane was employed as nonvolatile solvent. "As-prepared" samples (i.e., including the solvent) were used for biaxial experiments.

Fig. 2 shows the nominal biaxial stresses σ_x and σ_y for the end-linked PDMS elastomer of $\phi_0 = 0.70$ with as functions of the principal ratios λ_x and λ_y [23]. It should be emphasized that the stresses are the quasi-equilibrium ones with no appreciable time effect because they were obtained from the quasi-plateau stresses after sufficiently long time at each strain. It can be observed from the figure that the uniaxial stretching (triangular symbols; $\sigma_y = 0$) is only a part of the examined deformations. It should be noted that the uniaxial stretching data were obtained by another tensile tester using a rectangular strip of ca. 10 mm diameter and ca. 40 mm length which was cut from the sheet specimen used for biaxial measurements.

Using the biaxial data in Fig. 2, we assessed five entanglement models [26]: – the diffused-constraint model [31], the three different versions of the tube model [32–34], and the slip-link model [35,36]. We evaluated the structural parameters such as the numbers of elastically effective network strands and cross-links from the reaction conditions by using a nonlinear polymerization

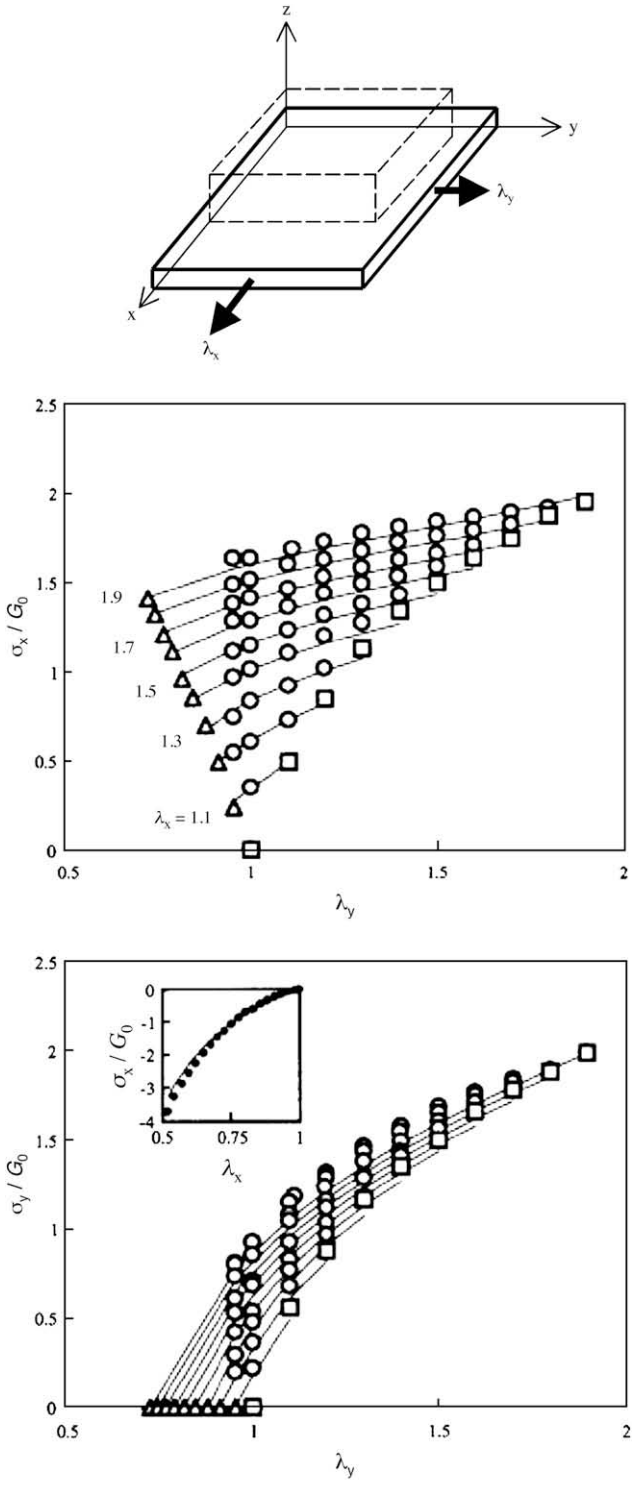

Fig. 2. Equilibrium nominal stresses σ_x and σ_y of an end-linked PDMS elastomer under various combinations of principal ratios λ_x and λ_y. The triangular symbols represent the data of uniaxial stretching. The inset indicates the data of uniaxial compression. The stresses are reduced by initial shear modulus to focus on the λ dependence of σ. The solid lines represent the best-fit result of the slip-link model. The data were reproduced from Refs. [23,26].

model [7], and used them in data fitting. In addition, the model-specific parameters were varied within the defined physically reasonable ranges. The details of the fitting results of each model are given in Ref. [26]. In conclusion, among the five models, the slip-link model provides the best description in the entire deformation. The solid lines in Fig. 2 depict the fitting results of the slip-link model. The slip-link theory models the trapped entanglements as mobile slip-links, and in addition, it considers the finite extensibility of network strands via the primitive path concept. The expression of elastic free energy (F_{el}) of the slip-link model is given by [35,36]

$$\frac{F_{el}}{RT} = \frac{1}{2}N_c\left[\frac{(1-\alpha^2)\sum\lambda_i^2}{1-\alpha^2\sum\lambda_i^2} + \ln\left(1-\alpha^2\sum\lambda_i^2\right)\right] + \frac{1}{2}N_s\left[\sum\left\{\frac{\lambda_i^2(1+\eta)(1-\alpha^2)}{\left(1+\eta\lambda_i^2\right)\left(1-\alpha^2\sum\lambda_i^2\right)} + \ln\left(1+\eta\lambda_i^2\right)\right\} + \ln\left(1-\alpha^2\sum\lambda_i^2\right)\right] \quad (1)$$

where $\sum$ denotes the summation for $i\,(=x,y,z)$, and N_c and N_s are the numbers of elastically effective network strands and slip-links, respectively. The model-specific parameters, η and α, characterize the slippage of the slip-link and the chain extensibility, respectively. The stresses in the figure are reduced by initial shear modulus (G_0) to focus on the comparison of the λ dependence of σ. The theoretical G_0 (=64.6 kPa) using the same parameter values in Fig. 2 excellently accords with the experimental value ($G_0 = 64.9$ kPa). Also, the value of G_0 is reasonably explained from the quasi-plateau modulus of uncrosslinked PDMS melt ($G_N^0 \approx 200$ kPa) [37] and the effective network concentration ($\phi_N = 0.62$) which is obtained by subtracting the unreacted soluble fraction from ϕ_0: $G_N^0(0.62)^a \approx 67$–77 kPa using $a = 2$–2.3 [38,39]. The slightly smaller value of the experimental G_0 may be due to the presence of a finite amount of dangling chains which have no contribution to equilibrium modulus. However, the agreement may also be considered tolerable in view of the uncertainty about the values of G_N^0 and a.

We compared further the predictions of the slip-link model with the biaxial data of the end-linked PDMS elastomers with different amounts of trapped entanglements prepared by varying ϕ_0 [27,28]. The quality of the fitting was found to be satisfactory, and the fitted results are given in Ref. [28]. Fig. 3 shows the ϕ_0 dependence of the entanglement contribution N_s/N_c, η and α. A decrease in ϕ_0 reduces N_s/N_c, which leads to an increase in η and a reduction in α. These trends agree with the expectation that a reduction in trapped

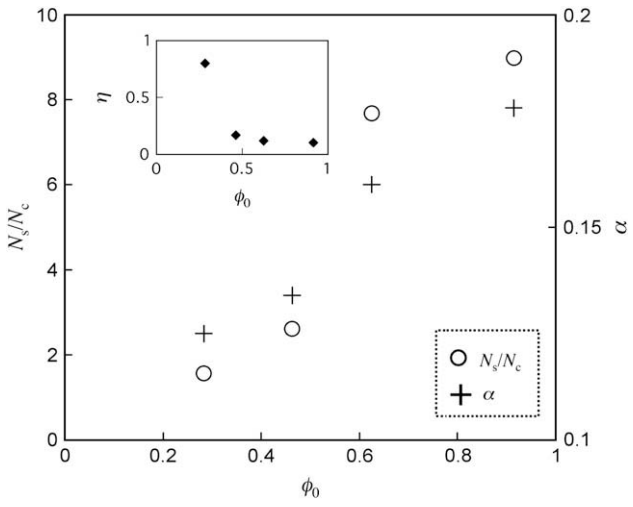

Fig. 3. The fitted parameters of the slip-link model as a function of ϕ_0. The data were reproduced from Ref. [28].

entanglements increases the slippage of the slip-links and extensibility (α^{-1}). Importantly, these model parameters are correlated with the topological characteristics of the networks by the relations $\eta \approx N_c/N_s$ and $\alpha^2 = N_j^{-1} = G_0 mp/(cRT)$ [35,36,40], where N_j, G_0, m, p, and c are the number of the Kuhn segments between topologically adjacent junctions, the small-strain shear modulus, the molecular mass of a repeating unit, the number of the repeating units per Kuhn segment, and the network (polymer) concentration, respectively. The values of η and α used in data fitting for each sample were compared with the corresponding values evaluated from the structural parameters in accordance with their definitions, independent of mechanical testing. The agreements between the two independent estimates were satisfactory for the widely accessible ranges $0 < \eta < \infty$ and $0 < \alpha < 1$ (see Table 2 in Ref. [28]). The slip-link model provides a good description of the biaxial data of these networks with the parameters of physically reasonable magnitudes. After the publications of our papers, some new entanglement theories [41–43] were proposed. However, the assessments using the biaxial data are not straightforward because some of the theories do not provide an analytical solution for the stresses under general biaxial strains due to their mathematical complexity.

We also estimated the phenomenological form of F_{el} as a function of the first and second invariants of the deformation gradient tensor on the basis of the derivatives of F_{el} with respect to each invariant which are obtained from the biaxial stress–strain data [23,27]:

$$F_{el}(I_1, I_2) = C_{10}(I_1 - 3) + C_{01}(I_2 - 3) + C_{11}(I_1 - 3)(I_2 - 3) + C_{20}(I_1 - 3)^2 + C_{02}(I_2 - 3)^2 \quad (2)$$

where $I_1 = \lambda_x^2 + \lambda_y^2 + \lambda_x^{-2}\lambda_y^{-2}$, $I_2 = \lambda_x^2\lambda_y^2 + \lambda_x^{-2} + \lambda_y^{-2}$ and C_{ij} are the numerical coefficients. It should be noticed that the extra three terms are needed to describe the data in addition to the familiar Mooney–Rivlin form [$F_{el} = C_{10}(I_1 - 3) + C_{01}(I_2 - 3)$]. The ϕ_0 dependence of each coefficient was discussed in Ref. [27].

3. Large-scale structure in the swollen state

Scattering measurements revealed the presence of a large-scale structure in swollen elastomers in solvents: this structure is absent in semi-dilute solutions of the corresponding uncrosslinked polymers with the same concentrations [44]. In the case of randomly crosslinked elastomers, this long-range structure is considered to originate from the heterogeneous distribution of cross-links. As compared to randomly crosslinked elastomers, the network strands in end-linked elastomers have uniform length. Bastide et al. [44,45] suggested that large-scale heterogeneity could arise even in end-linked networks due to "connectivity fluctuation", which qualitatively explains the excess scattering observed in several swollen end-linked elastomers [44–51]. However, most of these results were limited to end-linked elastomers comprising relatively short precursor chains with molecular weights comparable to or less than the critical molecular mass for entanglement formation (M_c). We investigated the small angle X-ray scattering spectra of the swollen end-linked PDMS elastomers comprising the precursors with M_p ranging from 2850 to 184,000 ($M_c \approx 17{,}000$ for PDMS) in order to elucidate the effect of entanglements on large-scale structure [49]. For all samples, the precursors were end-linked without solvents, and the resultant elastomers were allowed to swell fully in toluene (good solvent for PDMS).

Fig. 4 shows the M_p dependence of the scattering profiles of the swollen tetra-functional PDMS elastomers [49]. The scattering intensity (I) of each sample is reduced by the volume fraction of the elastomer in order to consider the difference in the degree of swelling. The scattering curves for seven different M_p are classified into two groups – $M_p > 23{,}800$ and $M_p < 12{,}800$. The value of M_c

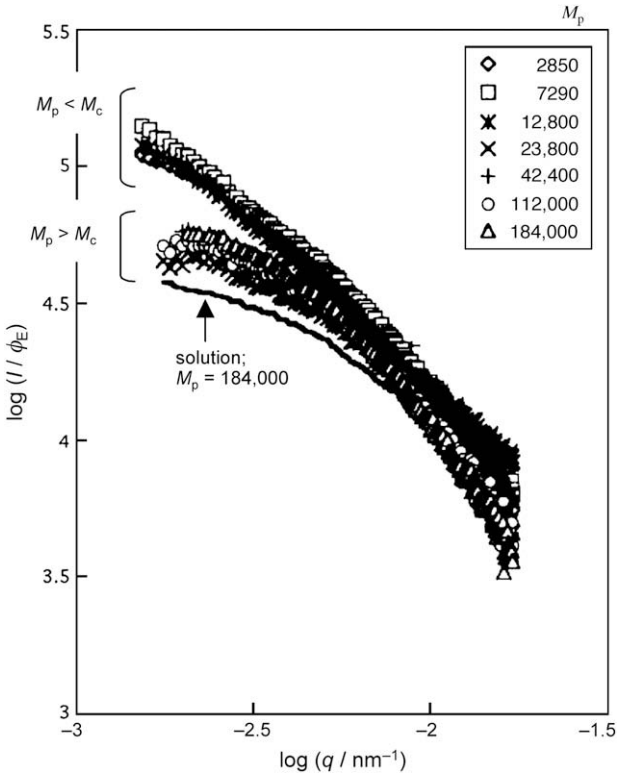

Fig. 4. The small angle X-ray scattering spectra of end-linked tetra-functional PDMS elastomers in the fully swollen state as a function of the molecular weight of the precursor (M_p). The scattering intensity (I) of each sample is reduced by the volume fraction of elastomer (ϕ_E). The data were reproduced from Ref. [49].

($\approx 17{,}000$) is within the boundary condition of M_p for the two types of scattering curves. This result indicates that the entangled state of the precursor chains before end-linking significantly affects the large-scale structure of the resultant elastomers in the swollen states, and the structures can be categorized into networks dominated by chemical cross-links and networks dominated by trapped entanglements. The scattering spectra of the networks with $M_p > M_c$ clearly level off in the small scattering vector (q) region. For a swollen network with $M_p = 184{,}000$, the excess scattering at small q is far lesser than that reported for various other swollen networks. This result shows that entanglement-dominated networks have a considerably uniform structure. Fig. 5 shows the M_p dependence of the characteristic length of the structure (Ξ), which is evaluated using the scattering data at low q using the Ornstein–Zernicke scattering function:

$$I(q) = \frac{I(0)}{1 + \Xi^2 q^2} \quad (3)$$

The values of Ξ drop significantly at around M_c, and the networks dominated by cross-links have more heterogeneous large-scale structures than entanglement-dominated networks. In Fig. 5 Ξ of each network is compared to the characteristic length (ξ) of the corresponding precursor solution having the same concentration. As M_p increases, the difference between Ξ and ξ becomes smaller, and they are almost similar in the region of $M_p > 10^5$. These results indicate that the spatially heterogeneous structure originates from chemical cross-links, thereby connectivity fluctuation; however such heterogeneity is effectively masked by the uniform entanglement networks when the mesh is dominated by entanglements. This is further supported by the following results [49]: a reduction in functionality of cross-links tends to increase Ξ, but such functionality effect on the large-scale structure is absent in the

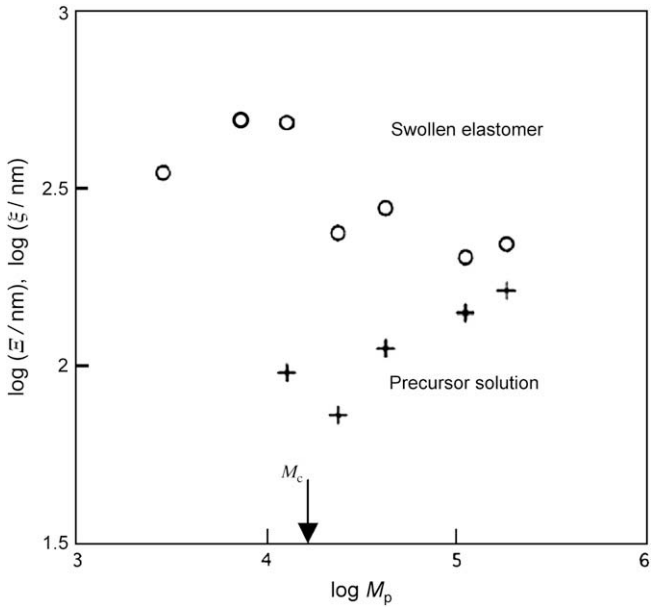

Fig. 5. The correlation lengths of the swollen end-linked PDMS elastomers and the corresponding uncrosslinked precursor solutions with the same concentrations as a function of the molecular weight of the precursor (M_p). The data were reproduced from Ref. [49].

elastomers of $M_p = 184{,}000$; the degree of size distribution of the precursor chains has no appreciable effect on the scattering profile of the swollen elastomers when the average molecular mass of the precursors is sufficiently larger than M_c. The effect of bimodal distribution of the length of precursor chains on the network structure was also investigated [51,52].

4. Marked extensibility in the highly deswollen state with "supercoil" network strands

The ultimate extensibility (λ_{max}) of a single polymer chain in the random coil state is given by $\lambda_{max} = N/N^{1/2} = N^{1/2}$ where N is the number of the constituent Kuhn segments [53]. This argument would indicate that a longer polymer chain is more extensible. However, highly extensible elastomers cannot be obtained by a mere end-linking of long precursor chains. This is because the end-linking of long precursors results in the formation of many trapped entanglements, which act as elastically effective cross-links. The "effective" length of network chains in such elastomers is governed by the distance between adjacent entanglements (N_e) and not by the size of the precursor (N). The value of N_e is specific to each polymer and is typically in the range of 20–40. The resultant λ_{max} ($N_e^{1/2} \approx 5$) roughly explains the empirical limitation of λ_{max} of conventional elastomers formed by cross-linking the precursors in the molten state. Obukhov et al. [54] theoretically proposed an interesting scheme to overcome such limitation of λ_{max}. Their scheme consists of two steps: (1) end-linking long precursors in the semi-dilute state; (2) deswelling the resultant gel to the dry state by removing the diluent. In the first step, as the precursor concentration (i.e., the degree of overlapping of the precursors) decreases, the resulting gel has a smaller amount of trapped entanglement. The second step induces a shrinkage in the conformation of network strands (i.e., a reduction in their end-to-end distance) due to a large reduction in the macroscopic volume of the gel. These two factors effectively enhance λ_{max}, and the effect becomes greater as the preparation concentration (ϕ_0) decreases [54]:

$$\lambda_{max} = N_{e,melt}^{1/2} \phi_0^{-23/24} \quad (4)$$

According to Eq. (4), the deswollen networks prepared at a low ϕ_0 (<0.03) exhibit a remarkable extensibility of $\lambda_{max} > 100$. The conformation of the network strands in the deswollen state is expected to become more compact than the corresponding Gaussian coil (random coil), termed "supercoil" [55,56]: the conformation of the network strands in the preparation state is the same as that of the Gaussian or excluded volume chain, and it is compressed further by large macroscopic shrinking of the gel upon deswelling. Several studies have investigated the mechanical properties of deswollen elastomers [57–59], but none of them have observed an appreciable enhancement in λ_{max}. This is primarily due to the relatively high ϕ_0 values used in their studies. It should be noted that the reduction in the macroscopic volume (leading to the compression of constituent network strands) upon deswelling increases with a decrease in ϕ_0.

Fig. 6 shows the nominal stress–elongation curves of the deswollen PDMS elastomer of a long precursor ($M_n = 99{,}000$) with a narrow size distribution ($M_w/M_n = 1.2$) prepared at $\phi_0 = 0.1$ [57]. For comparison, the data of the corresponding elastomer before deswelling and the elastomer prepared in the molten state ($\phi_0 = 1$) are also shown in the figure. The stress of each sample is normalized by the initial Young's modulus (E) of each sample. The deswollen elastomer is noticeably extensible up to $\lambda_{max} = 31$, while λ_{max} for the melt-crosslinked elastomer is only 2. The deswollen elastomer shows perfect strain recovery in unloading after elongation up to $\lambda = 25$. In addition to the marked extensibility, the unusually weak strain dependence of stress is characteristic of highly deswollen networks. Fig. 7 shows the double-logarithmic plots of nominal stress (σ) versus ($\lambda - \lambda^{-2}$). The λ dependencies of σ are classified into the three regions: $\sigma \sim (\lambda - \lambda^{-2})^{1.0}$ at small elongation of $\lambda < 2$; $\sigma \sim (\lambda - \lambda^{-2})^{0.46} \approx \lambda^{0.46}$ in the region of $2 < \lambda < 16$; and $\sigma \sim (\lambda - \lambda^{-2})^{1.0} \approx \lambda^{1.0}$ in the regime of $16 < \lambda < 31$. Pincus derived the scaling relation between σ and λ for a highly stretched single chain with a fractal dimension D: $\sigma \sim \lambda^{1/(D-1)}$ [56,61]. Such single chain approach will be applicable to the markedly extensible deswollen elastomers, because they are not expected to have any significant interaction between different network strands due to the low overlapping degrees of precursors in end-linking. According to Pincus blob scaling, a response in region II results in $D = 3.2$, which is considerably higher than $D = 2$ for the random coil. This indicates that the weak dependence in region II stems from the pull-out process of the compact conformation of network strands in the highly deswollen state.

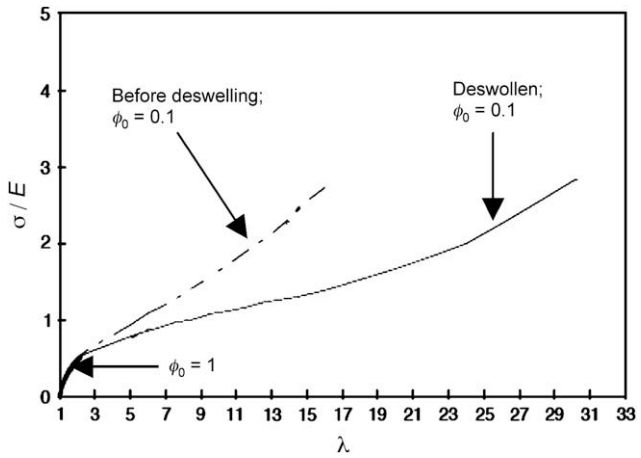

Fig. 6. The nominal stress–elongation curve of the deswollen PDMS elastomer with marked extensibility of $\lambda_{max} = 31$. The data of the corresponding elastomer before deswelling and the elastomer prepared in the melt are also shown. The stress of each sample is normalized by the initial Young's modulus. The data were reproduced from Ref. [60].

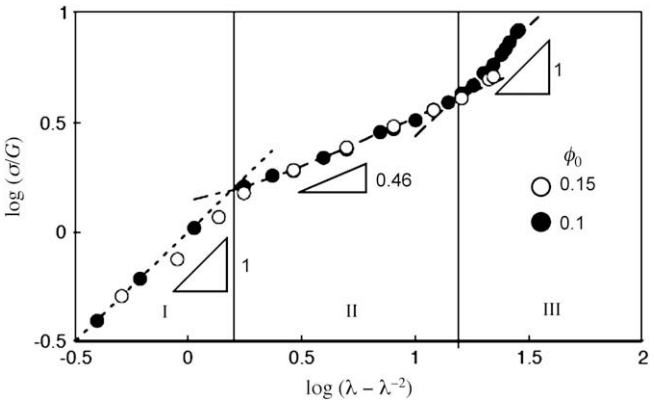

Fig. 7. Double-logarithmic plots of the nominal stress versus $(\lambda - \lambda^{-2})$ of the deswollen PDMS elastomers. The stress of each sample is normalized by the initial shear modulus. The data were reproduced from Ref. [60].

Interestingly, region III shows the response of random coil chains ($\sigma \sim \lambda^1$). It can be observed that the stretching drives the crossover from a supercoil to a random coil. Thus, region III shows the stretching process of the random coil formed due to the pulling out the compact conformation of supercoil. This type of crossover qualitatively accords with the prediction of Obukhov et al. [54]. The effects of supercoil formation were also observed in elastic modulus (E). The ϕ_0 dependence of E of the deswollen elastomers is far stronger than the prediction of classical theory ($E \sim \phi_0^{1/3}$) assuming the random coil even in the highly deswollen states [59,62]. The observed dependence [62] (approximated by $E \sim \phi_0^1$) is a matter of theoretical investigation, and a theory predicts the similar dependence [63].

Several studies showed the compressed conformation of supercoil and the unusual physical properties of the highly deswollen networks. A small angle neutron scattering experiment for the labeled network strands in the deswollen polystyrene gels revealed that the gyration radius was smaller than that observed in the unperturbed state [64]. In addition, it was observed that the compact conformation of the network strands in the highly deswollen state considerably affected the low-temperature crystallization behaviors of the elastomers [65]. Fig. 8 shows the ϕ_0 dependence of the enthalpy of fusion (ΔH_m) of the crystallines formed by cooling the deswollen PDMS elastomers to $-150\,^\circ$C. In the high ϕ_0 region of $\phi_0 > 0.2$, ΔH_m tends to increase with a decrease in ϕ_0. This is simply due to a reduction in the trapped entanglements acting as defects for crystallization. In contrast, ΔH_m of the highly deswollen elastomers at $\phi_0 < 0.2$ is lower than that at $\phi_0 \approx 0.2$. This implies that the compact conformation of the network strands in the highly deswollen state is disadvantageous to crystallization.

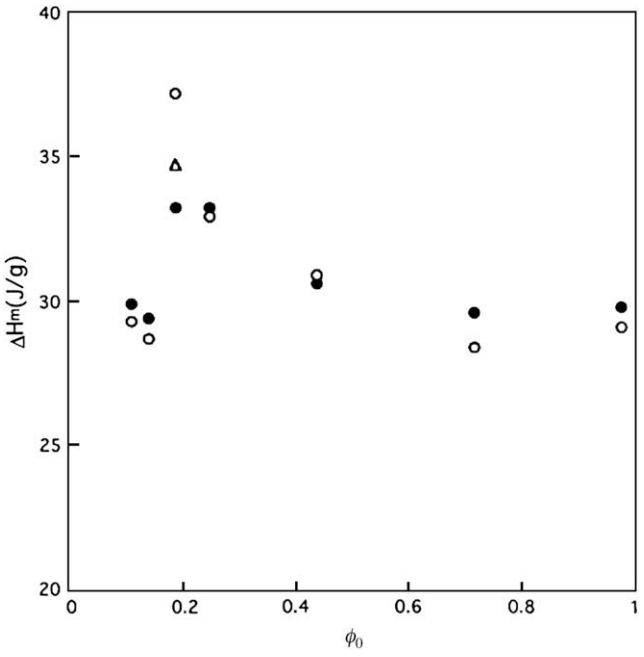

Fig. 8. Enthalpy of fusion of the crystallines formed by cooling to $-150\,^\circ$C in the deswollen PDMS elastomers prepared at various volume fractions of the precursor (ϕ_0). The closed and open symbols represent the data for cooling rates 9 and 200 $^\circ$C min^{-1}, respectively. The triangular symbol represents the data in which the contribution of crystallization during heating is subtracted. From Ref. [65].

5. Viscoelasticity of end-linked elastomers containing unattached linear chains or many dangling chains

5.1. Elastomers containing unattached linear chains

The viscoelastic behavior of elastomers containing small amounts of unattached chains has been investigated to characterize the dynamics of the polymer chains trapped in fixed networks [66–68]. Polymer chains trapped in fixed networks constitute a simpler system for the study of the polymer chain dynamics than the corresponding uncrosslinked polymer melts. This is because the complicated effect of the motion of the surrounding chains on the dynamics of the probe chain – called "constraint release" [69] – is absent in the fixed network systems. Most of the earlier studies employed randomly crosslinked elastomers as host networks. In this case, precise control of the mesh size of the host networks is not possible, and the mesh size has a broad distribution. The end-linking systems give the host networks a more uniform mesh size, and they can control the mesh size by the size of the precursor chains. We investigated the dynamic viscoelasticity of end-linked PDMS elastomers containing unattached linear PDMS as functions of the size of the unattached chains (M_g) and the network mesh (M_x) (Fig. 9a) [70]. We employed two types of host networks with $M_x > M_e$ and $M_x < M_e$ where M_e ($\approx$10,000 for PDMS) is the molecular mass between adjacent entanglements in the molten state. The $M_x > M_e$ and $M_x < M_e$ networks (designated as NL and NS, respectively) were designed by end-linking the long ($M_n = 84{,}000$) and short precursor chains ($M_n = 4{,}550$), respectively. The mesh of the NL networks is dominated by trapped entanglements, while that of the NS network is governed by chemical cross-links.

Fig. 9 shows the dynamic Young's modulus (E') and the loss tangent ($\tan\delta$) as a function of the angular frequency for NL containing unattached linear chains (15 wt%) with various M_g [70]. The time–temperature superposition principle was employed to construct the master curves. The mesh sizes of NL and NS were estimated to be $M_x = 1.2M_e$ and $M_x = 0.7M_e$ from the plateau values of E' in the low frequency limit, respectively. In the case of NL, M_x is greater than M_e ($M_x \neq M_e$) due to the dilution effect of the unattached chains on the entanglements. A definite peak of $\tan\delta$ resulting from the relaxation of the guest chains is observed. The peak position shifts to a lower frequency region as M_g increases. The characteristic time of the guest chains (τ) is evaluated as the inverse of the frequency at the peak position: $\tau \equiv 1/\omega_{\tan\delta,\max}$.

Fig. 10 shows the M_g dependence of τ for NL and NS. The dashed line for the data for NL corresponds to the M_g dependence of the longest relaxation time τ_L predicted by the reptation theory with the correction of the contour length fluctuation (CLF) of the tube [71,72]:

$$\tau_L = \frac{b^2\zeta_0 M_g^3}{M_x M_0^2 \pi^2 kT}\left[1 - 1.3\left(\frac{M_x}{M_g}\right)^{0.5}\right]^2 \qquad (5)$$

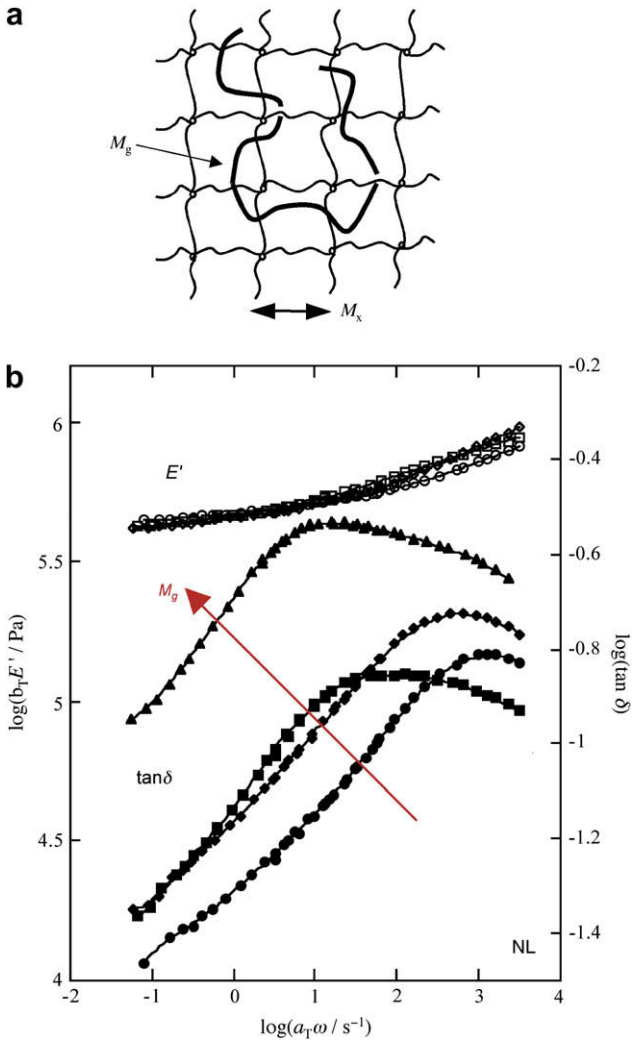

Fig. 9. (a) Free guest chain with the molecular weight of M_g trapped in the host network with a mesh size of M_x. (b) Frequency dependence of dynamic Young's modulus and loss tangent for the entanglement-dominated PDMS elastomers containing unattached linear PDMS with various molecular weights. E' data for the elastomer with no unattached chains are represented by crossed symbols, and the tan δ data lie outside the range of the figure due to the small magnitude. Weight-average molecular weight of the unattached PDMS (M_g): circle, 1.14×10^5; diamond, 1.38×10^5; rectangle, 2.85×10^5; triangle, 3.54×10^5 g/mol. The data were reproduced from Ref. [70].

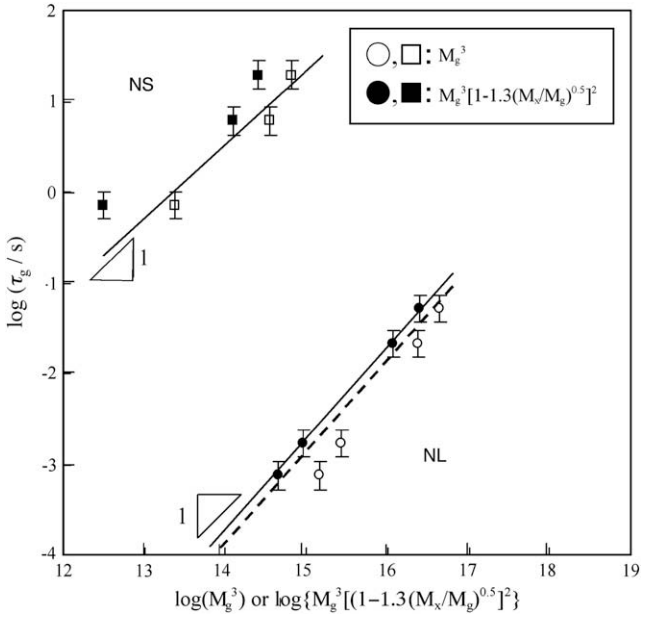

Fig. 10. Characteristic times τ_g of the unattached chains trapped in end-linked elastomers made of long ($M_p > M_e$) and short ($M_p < M_e$) precursors (designated as NL and NS, respectively) as a function of M_g. The dashed line depicts the prediction of Eq. (5). The data were reproduced from Ref. [70].

where b^2 is the mean-square end-to-end distance per monomer unit; ζ_0, the monomeric friction coefficient obtained from the viscous properties of PDMS melt; and M_0, the monomeric molar mass. The expression in brackets corresponds to the correction term for the CLF. In principle, τ evaluated from the tan δ peak is proportional, and not identical, to τ_L. As observed in Fig. 10, the value of τ for NL is slightly larger but close to the value of τ_L calculated from Eq. (5). The M_g dependence of τ for NL ($\tau \sim M_g^{3.6}$) is stronger than the cubic power law expected by the original reptation model [72]. The results for NL are more satisfactorily described by the prediction of the tube model with CLF correction. The M_g dependence of τ for NS obeys the cubic power law. The M_g dependence of τ is well described within the framework of the reptation theory independently of M_x.

More interestingly, the effect of the mesh size on τ is unexpectedly large: the value of τ for NS is far larger than that for NL (by a factor of nearly 10^5). According to Eq. (5), τ increases with a decrease in M_x, which was called the "strangulation" effect [73]. The effect of M_x in Eq. (5) ($\tau \sim M_x^{-1}$), however, is too small to explain such a large difference in τ. It should be noted that the meshes of NL and NS are different in not only size but also in character: NL and NS are dominated by entanglements and cross-links, respectively. An NMR study [74] on end-linked PDMS elastomers with varying M_p revealed that the mobility of the network strands decreases significantly when M_p is less than M_e. This difference in the mobility of the host rubber matrix is expected to influence the dynamics of the guest chains. However, the difference in the mobility of host matrix was not recognizable in the horizontal shift factor (a_T) in the time-temperature superposition principle. The values of a_T for NL and NS were the same. The difference in mesh character between the host networks with $M_x > M_e$ (entanglement-dominant) and $M_x < M_e$ (crosslink-dominant) is unavoidable in the experiments with M_x varying across M_e. This prevents us from exclusively observing the strangulation effect of tight networks without the influence of mesh characters in the region of $M_x < M_e$.

The dynamics of guest chains with different architectures in fixed networks has also been investigated. Stress relaxation behaviors were examined for end-linked elastomers with a low concentration of star-shaped chains [75] and dangling chains (those tethered to the network at only one end) [10,76]. They exhibit similar broad relaxation spectra because the center of mass of the star-shaped chains is almost immobile in host networks [75].

5.2. Elastomers containing many dangling chains

Dangling chains – attached to networks at only one end – are defects in the network structures. Elastomers with many dangling chains have irregular network structures composed of many branched parts with a wide size distribution (Fig. 11a). The mechanical damping of such irregular networks is expected to become large and insensitive to frequency and temperature: the dangling chains with free ends dissipate the applied work as heat energy by viscoelastic relaxation, and the branched structures with wide size distributions have broad relaxation spectra due to their numerous types of relaxation modes. In contrast, perfect networks without dangling chains can store the entire imposed work as elastic energy. The end-linking reaction provides irregular elastomers with known amounts of dangling chains, thereby enabling the study of

the correlation between structural irregularity and viscoelasticity [4,7,77].

We prepared irregular PDMS elastomers via two different schemes [78]: in scheme A, mixtures of mono- and bi-functional precursors (with $M_n = 29{,}600$ and 25,700, respectively) with different mixing ratios were end-linked using tri-functional cross-linkers at the stoichiometric ratio ($r = 1$ where r is the molar ratio of the Si–H groups in the cross-linker to the vinyl groups in the precursors); in scheme B, the bi-functional precursors were end-linked with tri-functional cross-linkers at different mixing ratios, i.e., off-stoichiometric ratios ($r > 1$ and $r < 1$). After the reaction, the soluble species were extracted by swelling the resultant elastomers in toluene. A fraction of pendent parts (W_{pen}) was evaluated by the nonlinear polymerization theory and the weight fraction of the soluble species. Dynamic viscoelastic measurements were made for the elastomers (containing no soluble species) dried after the extraction procedure. Some earlier studies [4,79] reported the dynamic viscoelasticity of some irregular elastomers, but none of them removed large amounts of extractable materials (i.e., the material which is not incorporated into the infinite network). The extractable materials also behave as relaxation component when they are sufficiently large, as shown in the last section. The extraction of the soluble species is needed to observe the damping performance that originates purely from the irregularity of infinite networks.

Fig. 11 shows the temperature dependence of tan δ and E' for irregular elastomers prepared by scheme B for different r values [78]. The excess conditions of cross-linker and precursor correspond to $r > 1$ and $r < 1$, respectively. The most regular elastomer

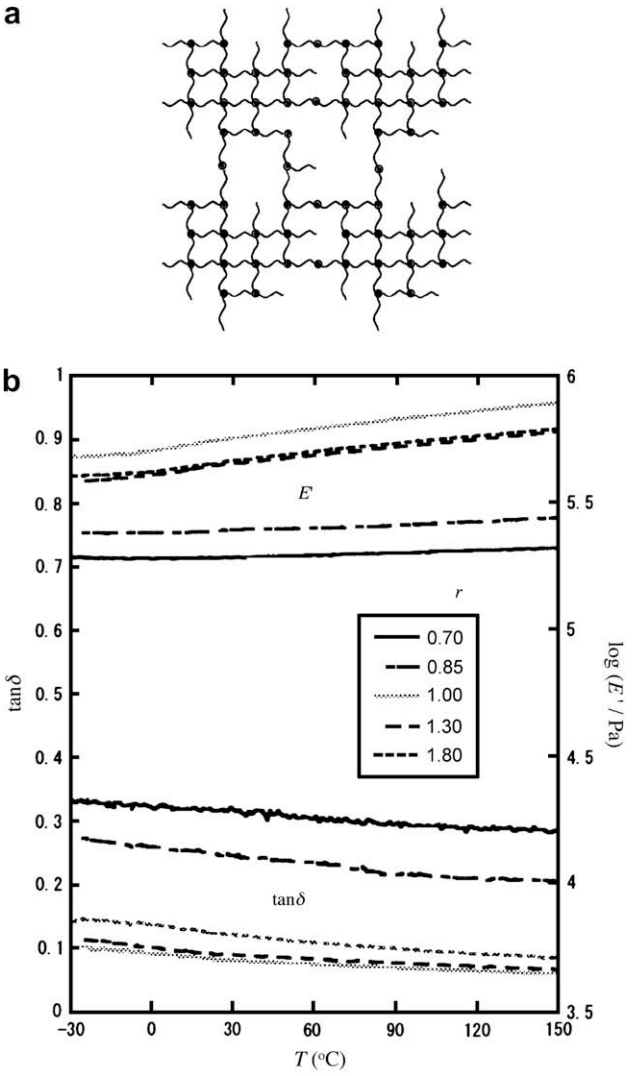

Fig. 11. (a) Irregular networks containing many dangling chains. (b) Temperature dependence of loss tangent and the dynamic Young's modulus for the irregular PDMS elastomers prepared for various ratios of mixtures of bi-functional precursor and tri-functional cross-linker. The stoichiometric condition corresponds to $r = 1$, while the excess condition of the precursor (cross-linker) is $r < 1$ ($r > 1$). The data were reproduced from Ref. [78].

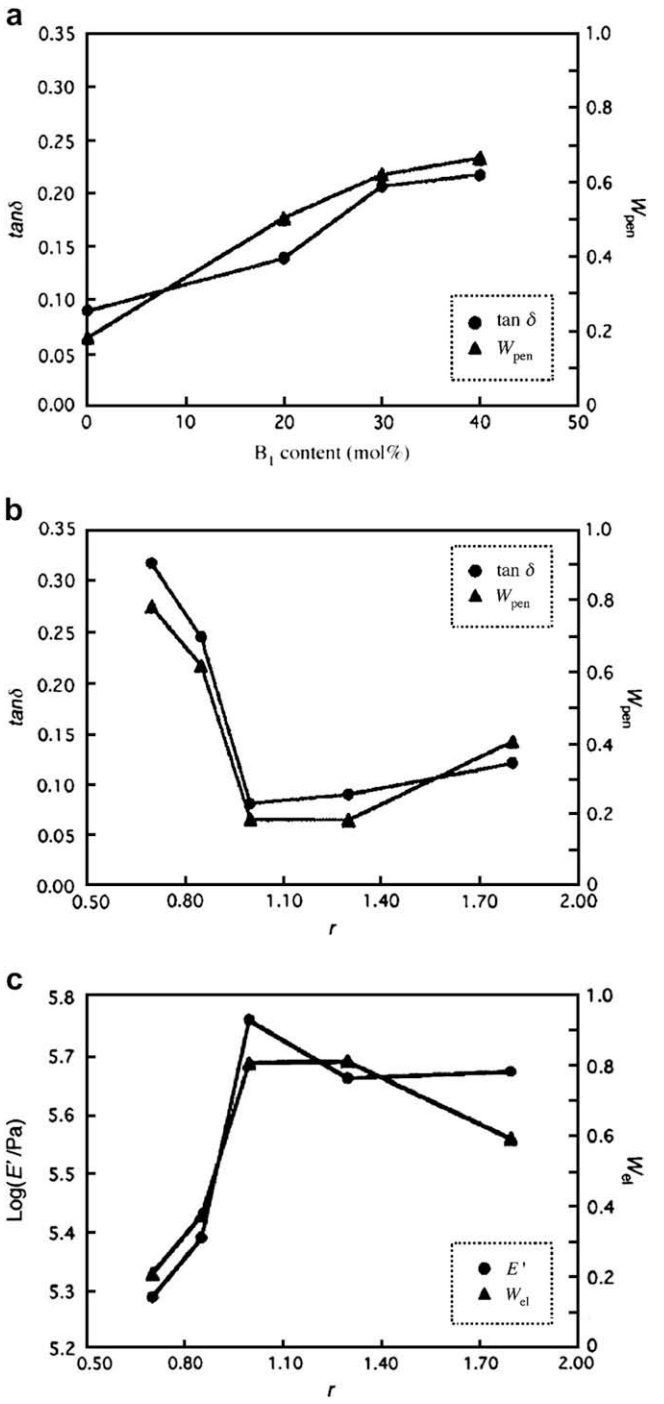

Fig. 12. (a) Correlation of loss tangent and the fraction of pendent parts for irregular PDMS elastomers obtained via scheme A as a function of the content of the mono-functional precursor (B_1). (b) Correlation of the loss tangent and the fraction of the pendent parts for the irregular PDMS elastomers via scheme B at various r. (c) Correlation of the dynamic Young's modulus and the fraction of elastically effective parts for irregular PDMS elastomers obtained via scheme B at various r. The data were reproduced from Ref. [78].

with $r = 1.0$ exhibits a small tan δ value less than 0.1. In contrast, the most excessive condition of precursor ($r = 0.7$) results in high damping elastomers showing tan $\delta > 0.3$ in a wide temperature range of $-30\,^{\circ}\mathrm{C} < T < 150\,^{\circ}\mathrm{C}$. The storage modulus E' at $r = 0.7$ shows no significant T dependence, which indicates that the elastomer is in a rubbery state in the entire T range examined, and high damping does not originate from any structural transition.

Fig. 12 shows the correlation between the viscoelastic and structural parameters for irregular elastomers [78]. In scheme A, tan δ increases with the content of mono-functional precursor in the reactant mixtures. The highest content of mono-functional precursor (40 mol%) leads to the highest damping (ca. 0.25) among the samples via scheme A. Evidently, tan δ and W_{pen} are strongly correlated, and damping results from the viscoelastic relaxation of the dangling parts. In addition, it is observed that E' increases with the fraction of elastically effective network backbone W_{el} ($= 1 - W_{\mathrm{pen}}$). These tendencies are commonly observed for elastomers via schemes A and B, i.e., independent of the preparation method. These results clearly indicate that the network elasticity originates from the network backbone while the dissipativity of networks originates from the dangling parts. In the case of elastomers with the highest damping ($r = 0.7$), W_{el} is only 0.2, and most parts of the network belong to dangling parts. No macroscopic gelation occurred at $r < 0.7$. The damping that stems from structural irregularity is also insensitive to frequency [78]. This is expected because of the independence of T. It should be noted that the utilization of structural irregularity for damping is universal for general elastomers and is not just limited to PDMS. In addition, high damping arising from similar types of structural irregularities was reported for elastomers other than PDMS [80].

6. Summary

We have shown that end-linked elastomers with a controlled network topology provide a model system that can enable the comprehension of the structure–mechanical properties' relationships of polymer networks on a molecular basis. The nonlinear stress–strain relations under general biaxial strains for model elastomers with well-characterized structures give an unambiguous basis to strictly assess the molecular entanglement theories. Small angle X-ray scattering of swollen model elastomers revealed the roles of chemical cross-links and entanglements in the large-scale network structures of the swollen states. The markedly stretchable elastomers with topological features which are optimized for extensibility – i.e., having few trapped entanglements and compact conformation of network strands – were prepared by end-linking long precursors in semi-dilute solutions and subsequently drying (deswelling) the gels. End-linked networks containing unattached chains exhibited high damping at a certain frequency: the origin of this damping is the viscoelastic relaxation via reptative motion of the guest chains. The characteristic frequency can be controlled by the size of the guest chains and the mesh size. Irregular networks containing many dangling chains lead to the formation of elastomers with high damping. This damping is insensitive to temperature and frequency changes due to the broad size distribution of pendent parts.

Elastomers with tailored topological characteristics provide a definite basis for the molecular understanding of the fundamentals of physicochemical properties of flexible polymer networks. We also expect that controlling the network topology possesses a further potential to enhance the performance of elastomers.

Acknowledgments

The authors wish to express their sincere gratitude to Keisuke Yokoyama and Takashi Miki for their contributions to the experiments. The authors also thank Prof. T. Takigawa of Kyoto University for facilitating a helpful discussion. This work was partly supported by a Grant-in-Aid for Scientific Research (B) (No. 16750186) and a Grant-in-Aid on Priority Area "Soft Matter Physics" (No. 19031014) from the Ministry of Education, Culture, Sports, Science and Technology (MEXT) of Japan. This research was also supported in part by the Global COE Program "International Center for Integrated Research and Advanced Education in Materials Science" (No. B-09) of MEXT of Japan, administrated by the Japan Society for the Promotion of Science.

References

[1] Treloar LRG. The physics of rubber elasticity. 3rd ed. Oxford: Clarendon Press; 1975.
[2] Mark JE, Erman B. Rubberlike elasticity: a molecular primer. 2nd ed. Cambridge: Cambridge University Press; 2007.
[3] Gottlieb M, Macosko CW, Benjamin GS, Meyers KO, Merrill EW. Macromolecules 1981;14:1039–46.
[4] Patel SK, Malone C, Cohen C, Gillmor JR, Colby RH. Macromolecules 1992;25:5241–51.
[5] Erman B, Mark JE. Structures and properties of rubberlike networks. New York: Oxford University Press; 1997.
[6] Larsen AL, Sommer-Larsen P, Hassager O. e-Polymers 2004:050.
[7] Miller DR, Macosko CW. Macromolecules 1976;9:206–11.
[8] Llorente MA, Andrady AL, Mark JE. J Polym Sci Part B Polym Phys 1981;19:621–30.
[9] Madkour T, Mark JE. Polym Bull 1993;31:615–21.
[10] Vega DA, Villar MA, Alessandrini JL, Valles EM. Macromolecules 2001;34:4591–6.
[11] Candau S, Peters A, Herz J. Polymer 1981;22:1504–10.
[12] Urayama K, Kohjiya S. J Chem Phys 1996;104:3352–9.
[13] Urayama K, Kawamura T, Kohjiya S. J Chem Phys 1996;105:4833–40.
[14] Stepto RFT. In: Clarson SJ, Semlyen JA, editors. Siloxane polymers. New Jersey: Prentice Hall; 1993. p. 373–414.
[15] Tschoegl NW, Gurer C. Macromolecules 1985;18:680–7.
[16] Urayama K. J Polym Sci Part B Polym Phys 2006;44:3440–4.
[17] James AG, Green A, Simpson GM. J Appl Polym Sci 1975;19:2033–58.
[18] Tsuge K, Arenz RJ, Landel SJ, Landel RF. Rubber Chem Technol 1978;51:948–58.
[19] Kawabata S, Matsuda M, Tei K, Kawai H. Macromolecules 1981;14:154–62.
[20] Kawabata S, Kawai H. Adv Polym Sci 1977;24:89.
[21] Gottlieb M, Gaylord RJ. Macromolecules 1987;20:130–8.
[22] Fukahori Y, Seki W. Polymer 1992;33:502–8.
[23] Kawamura T, Urayama K, Kohjiya S. Macromolecules 2001;34:8252–60.
[24] Kawamura T, Urayama K, Kohjiya S. Reoroji Gakkaishi (J Rheol Soc Jpn) 2003;31:213–7.
[25] Gottlieb M, Gaylord RJ. Polymer 1983;24:1644–6.
[26] Urayama K, Kawamura T, Kohjiya S. Macromolecules 2001;34:8261–9.
[27] Kawamura T, Urayama K, Kohjiya S. J Polym Sci Part B Polym Phys 2002;40:2780–90.
[28] Urayama K, Kawamura T, Kohjiya S. J Chem Phys 2003;118:5658–64.
[29] Orrah DJ, Semlyen JA, Rossmurphy SB. Polymer 1988;29:1452–4.
[30] Macosko CW, Benjamin GS. Pure Appl Chem 1981;53:1505–18.
[31] Kloczkowski A, Mark JE, Erman B. Macromolecules 1995;28:5089–96.
[32] Gaylord RJ, Douglas JF. Polym Bull 1990;23:529–33.
[33] Kaliske M, Heinrich G. Rubber Chem Technol 1999;72:602–32.
[34] Rubinstein M, Panyukov S. Macromolecules 1997;30:8036–44.
[35] Edwards SF, Vilgis T. Polymer 1986;27:483–92.
[36] Edwards SF, Vilgis TA. Rep Prog Phys 1988;51:243–97.
[37] Plazek DJ, Dannhauser W, Ferry JD. J Colloid Sci 1961;16:101–26.
[38] Isono Y, Fujimoto T, Takeno N, Kajiura H, Nagasawa M. Macromolecules 1978;11:888–93.
[39] Takahashi Y, Noda I, Nagasawa M. Macromolecules 1985;18:2220–5.
[40] Vilgis TA, Erman B. Macromolecules 1993;26:6657–9.
[41] Mergell B, Everaers R. Macromolecules 2001;34:5675–86.
[42] Rubinstein M, Panyukov S. Macromolecules 2002;35:6670–86.
[43] Xing XJ, Goldbart PM, Radzihovsky L. Phys Rev Lett 2007;98:075502.
[44] Bastide J, Candau SJ. Structure of gels as investigated by means of static scattering techniques. In: Cohen JP, editor. Physical properties of polymeric gels. Chichester: John Wiley & Sons Ltd.; 1996. p. 143–308.
[45] Rouf-George C, Munch JP, Beinert G, Iset F, Pouchelon A, Palierne JF, et al. Polym Gels Networks 1996;4:435.
[46] Mendes E, Girard B, Picot C, Buzier M, Boue F, Bastide J. Macromolecules 1993;26:6873–7.
[47] Geissler E, Horkay F, Hecht AM. J Chem Phys 1994;100:8418–24.
[48] Shibayama M, Takahashi H, Nomura S. Macromolecules 1995;28:6860–4.
[49] Kawamura T, Urayama K, Kohjiya S. J Chem Phys 2000;112:9105–11.
[50] Sukumaran SK, Beaucage G, Mark JE, Viers B. Eur Phys J E 2005;18:29–36.
[51] Urayama K, Kawamura T, Hirata Y, Kohjiya S. Polymer 1998;39:3827–33.
[52] Viers BD, Mark JE. J Inorg Organomet Polym Mater 2005;15:477–83.
[53] Kuhn W. J Polym Sci 1946;1:380–8.
[54] Obukhov SP, Rubinstein M, Colby RH. Macromolecules 1994;27:3191–8.
[55] Dusek K, Prins W. Adv Polym Sci 1969;6:1.
[56] de Gennes PG. Scaling concepts in polymer physics. New York: Cornell University Press; 1979.

[57] Johnson RM, Mark JE. Macromolecules 1972;5:41.
[58] Ong CSM, Stein RS. J Polym Sci Part B Polym Phys 1974;12:1599–606.
[59] Vasiliev VG, Rogovina LZ, Slonimsky GL. Polymer 1985;26:1667–76.
[60] Urayama K, Kohjiya S. Eur Phys J B 1998;2:75–8.
[61] Pincus P. Macromolecules 1976;9:386–8.
[62] Urayama K, Kohjiya S. Polymer 1997;38:955–62.
[63] Rubinstein M, Panyukov S. Private communication.
[64] Bastide J. In: Boccara N, Daoud M, editors. Physics of finely divided matter. Berlin: Springer; 1985.
[65] Urayama K, Yokoyama K, Kohjiya S. Polymer 2000;41:3273–8.
[66] Granick S, Pedersen S, Nelb GW, Ferry JD, Macosko CW. J Polym Sci Part B Polym Phys 1981;19:1745–57.
[67] Poh BT, Adachi K, Kotaka T. Macromolecules 1987;20:2569–74.
[68] Ndoni S, Vorup A, Kramer O. Macromolecules 1998;31:3353–60.
[69] Klein J. Macromolecules 1986;19:105–18.
[70] Urayama K, Yokoyama R, Kohjiya S. Macromolecules 2001;34:4513–8.
[71] Doi M. J Polym Sci Part C Polym Lett 1981;19:265–73.
[72] Doi M, Edwards SF. The theory of polymer dynamics. Oxford: Oxford University Press; 1986.
[73] de Gennes PG. Macromolecules 1986;19:1245–9.
[74] Callaghan PT, Samulski ET. Macromolecules 2000;33:3795–802.
[75] Vega DA, Gomez LR, Roth LE, Ressia JA, Villar MA, Valles EM. Phys Rev Lett 2005;95:166002.
[76] Batra A, Cohen C, Archer L. Macromolecules 2005;38:7174–80.
[77] Larsen AL, Hansen K, Sommer-Larsen P, Hassager O, Bach A, Ndoni S, et al. Macromolecules 2003;36:10063–70.
[78] Urayama K, Miki T, Takigawa T, Kobjiya S. Chem Mater 2004;16:173–8.
[79] Bibbo MA, Valles EM. Macromolecules 1984;17:360–5.
[80] Patil HP, Hedden RC. J Polym Sci Part B Polym Phys 2007;45:3267–76.

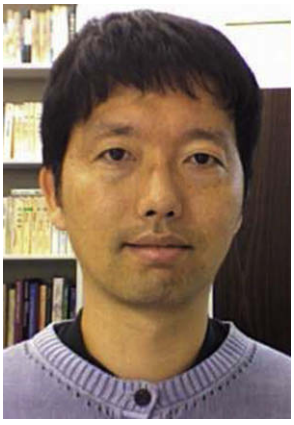

Kenji Urayama is an Associate Professor of Materials Chemistry at Kyoto University. He completed the undergraduate course of Polymer Chemistry at Kyoto University, and also earned his Ph.D. at Kyoto University in 1996. Urayama was an Assistant Professor of the Institute for Chemical Research at Kyoto University in 1994–2003. He did a post-doctoral fellow at Max-Planck-Institute for Polymer Research in 1998. His research interest focuses on the stimulus–response behaviors of polymer gels and elastomers including liquid crystal elastomers. His awards include the John H. Dillon Medal (Division of Polymer Physics in American Physical Society, 2006) and the SPSJ Wiley Award (The Society of Polymer Science, Japan, 2007).

Takanobu Kawamura is an assistant professor of Chemical Engineering in Kanazawa University. He obtained his Ph.D. at Kyoto University in 2001. After finishing his Ph.D. studies, Kawamura got the Research Fellowship for Young Scientist (PD) from the Japan Society for the Promotion of Science at Kyoto Institute of Technology in 2001–2004. His present research interests focused on the relationship between structure and mechanical properties of polymeric materials including plastics and rubbers. He got the Award for Encouragement of Research in Polymer Science from the Society of Polymer Science, Japan (2008).

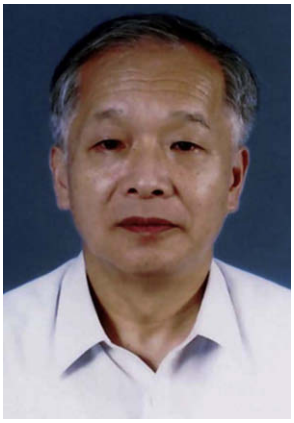

Shinzo Kohjiya is a Professor Emeritus of Kyoto University, and currently a Visiting Professor in Faculty of Science at Mahidol University in Thailand. He completed the undergraduate course of Polymer Chemistry at Kyoto University, and also gained his Ph.D. at Kyoto University. Kohjiya was an Assistant Professor in Faculty of Engineering and Design at Kyoto Institute of Technology (KIT) in 1969–1977, Associate Professor in 1977–1991 and promoted to Professor in the same faculty of KIT in 1991. In 1993 he moved to the Institute for Chemical Research at Kyoto University as a Professor. He was a Visiting Professor of Mapua Institute of Technology in Philippines after his retirement from Kyoto University in 2006. His research interests cover the fabrications and characterizations of the high-performance and high-functionality elastomers. His honors include the Oenslager Award (Chemical Society of Japan and Society of Rubber Industry, Japan, 1994).